AGEING EFFECTS ON HIGH DAMPING BRIDGE RUBBER BEARING

Haosheng Gu and Yoshito Itoh
Department of Civil Engineering, Nagoya University
E-mail: hausn@civil.nagoya-u.ac.jp

ABSTRACT: In recent years high damping rubber (HDR) material has attracted much attention of technologists because it possesses both flexibility and high damping properties. However, it is also known that rubber performance drops due to the ageing effect. Many problems are still not clear, for example, how does the property of HDR material change over the time, which environmental factor dominates the degradation of HDR, in what way does ageing progress from the surface to the interior of the HDR bearing, and what influence does ageing produce on the mechanical performance of HDR bridge bearing. In order to solve these problems, in this study a series of accelerated exposure tests are carried out on HDR pieces and blocks. Firstly, different degradation factors such as thermal oxidation, ultraviolet, ozone, low temperature ozone, salt water and acid rain are applied to HDR specimens. The property variations are examined and the thermal oxidation is found to be the predominant degradation factor. Then, thermal oxidation tests are performed on HDR blocks at various elevated temperatures and the development of the property profiles is investigated. An aging model for HDR bearing is developed to predict the mechanical behaviors at any position inside the bearing. Next, based on the predicted material properties, FEM analysis is carried out using the constitutive law. Finally, the long-term performance of aged HDR bearing is clarified. Using the Arrhenius methodology, the test conditions may be transformed to the real environment, so that the future performance a HDR bridge bearing may be estimated with the site condition taken into consideration.

Keywords — High damping rubber, aging, thermal oxidation, long-term performance

1. INTRODUCTION

In order to reduce the damage suffered by bridges during a severe earthquake, base isolation devices have come into wide use. Rubber is frequently applied in bridge bearings because of its special properties such as high elasticity and large elongation at failure. However, natural rubber cannot afford sufficient damping which is indispensable to a seismic isolation system. Usually rubber bearings have to be used together with damping devices such as steel bars, lead plugs, etc. Therefore in the early 1980's high damping rubber (HDR) was invented. HDR material possesses both flexibility and high damping properties, so that the bridge bearings made of HDR can not only extend the natural period of the bridge, but also reduce the displacement response of structures. Moreover, because of the inherent high damping characteristics of HDR, additional devices become unnecessary, so that the seismic isolation system is made more compact.

Many studies have been carried out on the static and dynamic behavior of HDR materials. Yoshida et al. (2004) developed a mathematical model of HDR materials and proposed a three-dimensional finite element modeling methodology to simulate the behaviors of a HDR bearing numerically. The ageing problems of HDR have also been studied in recent years. For the purpose of clarifying the deterioration characteristics of a bridge rubber bearing during its lifespan, some bearings practically in use were recalled and their mechanical properties were tested (Sudoh et al., 2003). However, because of their scattered nature and the lack of data, the degradation mechanism and the long-term performance of HDR are still not very clear. During the design process, usually the behaviors of aged bridge rubber bearings during their lifespan are not considered.

In this research, through accelerated exposure tests using various environmental factors, the aging characteristics of HDR is investigated and the dominant degradation factor is determined. Then accelerated tests using the most significant degradation factor are performed on HDR blocks. The deterioration profiles of the HDR blocks are studied at different elevated temperatures. Based on the test results, and heterogeneous property profiles of aged HDR bearing could be predicted using an aging model. Next, the material properties are applied to the FEM model and the long-term mechanical performances of an aged HDR bearing are examined with the site environment conditions taken into consideration. The HDR specimens are provided by Tokai Rubber Industries, Ltd. It is possible that when suffered by aging, the HDR from other companies may behave differently due to the difference of the chemical compound. The deterioration characteristics of the HDR material with other compounding ingredients and additives will be discussed in the future study.

2. ACCELERATED EXPOSURE TESTS ON HDR MATERIAL

2.1 Specimens and Test Methods

Firstly, accelerated exposure tests are performed to observe the aging behaviors of HDR material under various degradation conditions. In all the tests, the No.3 dumbbell specimens specified by JIS K 6251 are used. As shown in **Fig.1**, the dumbbell-like specimen with a thickness of 2 mm is designed for the tensile test. The middle part with a width of 5 mm and a length of 20 mm is applied to evaluate the deterioration characteristics. The samples are sufficiently thin to avoid diffusion-limited oxidation effects during the experiment. Since the outer surface of the rubber layer between steel plates will bloom outwards when the bearing subjected to the compressive dead and live loads, the specimens are stretched to certain strains using a special rig shown as **Fig.2**. In the test the pre-strains are set as 0%, 20% and 40% to investigate the influence of the combinations of tensile strain and degradation factors. For each degradation factor, each pre-strain state and each measuring time, 12 samples are prepared.

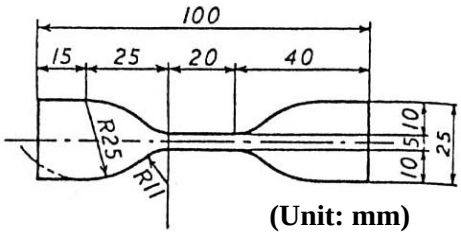

Fig.1 JIS No.3 dumbbell pecimen

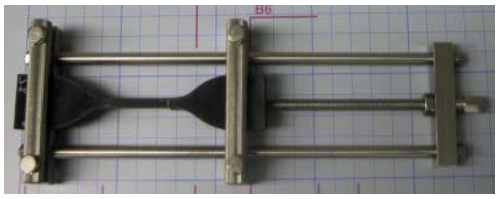

Fig.2 Pre-straining rig

Table 1 Conditions of accelerated ageing test

Degradation factor	Test condition	Time (hours)
Thermal oxidation	70	96, 192, 384, 768, 1536, 3072, 6144
Ozone	Ozone=0.5ppm, 40	96, 192, 384, 768, 1536
Low-temperature ozone	Ozone=0.5ppm, -30	96, 192, 384, 768, 1536
Ultraviolet radiation	Radiation and water spray	360, 720, 1440
Salt water spray	Wetting and drying cycle	360, 720, 1440
Acid rain spray	Wetting and drying cycle	360, 720, 1440

In this research, six kinds of environmental conditions are simulated by the accelerated exposure tests listed in **Table 1**. They are thermal oxidation test, 40□ ozone deterioration test, low-temperature ozone deterioration test, weather resistant test, salt water mist combined cycle test and acid rain mist combined cycle test. The thermal oxidation test is carried out in a temperature-controlled air-ageing oven, and the ambient temperature is kept as 70□. The ozone test method conforms to JIS K 6259 with the concentration of ozone being 0.5ppm and the environmental temperature being 40□. In the low-temperature ozone test the temperature is set as -30□. The weather resistant accelerated test is to examine the influence of the sunlight irradiating the rubber material. The cycle composed of 60 minutes of irradiation and 30 minutes of pure water spaying is adopted. The salt water mist combined cycle test uses the S6-cycle, which is proposed by the Ministry of International Trade and Industry and is specified in JIS K 5621. The S6-cycle consists of 30 minutes of salt water spraying (30±2□, 98%), 90 minutes of wetting (30±2□, 95%), 120 minutes of drying by hot wind (50±2□, 20%), 120 minutes of drying by warm wind (30±2□, 20%). The acid rain mist combined cycle test just replaces the 5% salt water by pH3.5 acid fluid and keeps other conditions unchanged, and the acid fluid is made from sulfuric and nitric acid. The conditions in the accelerated exposure tests are much severer than the real environment in order to investigate the long-term characteristics within the limited time.

The uniaxial tensile experiment is performed to investigate the mechanical properties of the aged rubber specimens. The inspection method conforms to the specifications in JIS K6251 and K6253 about the general rules of physical testing methods for vulcanized rubber. Because the stress-strain relationship of rubber material shows high non-linearity, it is difficult to calculate the stiffness using the secant method. For all the aged rubber samples, the stresses at 25%, 50%, 100%, 200% and 300% strain, i.e. M25, M50, M100, M200 and M300, the elongation at break (EB) and tensile strength (TS) are taken as the evaluation indexes. The average values with the double of the standard deviations (M±2S) are illustrated.

2.2 Test Results and Discussions

Fig.3 shows the degradation effects on HDR. In **Fig.3(a)**, the thermal oxidation test results show the continuous change of M100, EB and TS. At 6,144 hour, M100 is already 2.25 times of the initial value, and there are only 25% of EB and 50% of TS left. Ozone deterioration does not influence the HDR properties much, with an increase of M100 and a decrease of EB by about 20% after 1,536 hours, respectively. In the low-temperature ozone test, the material properties do not change at all (**Fig.3(b)**, **(c)**). In the ultraviolet radiation test, after about 700 hours the increase speed of M100 slows down and approaches to 50%, as shown in **Fig.3(d)**. In the salt water mist combined cycle test, the stable state is reached in 400 hours. From **Fig.3(e)** it is found that M100 increases 35%, and EB decreases 25%, while TS seems to almost have no decrease by the end of the test. **Fig.3(f)** shows that the property changes due to the acid rain mist combined cycle are not very large, either. After 1,440 hours M100 increases 30%, EB decreases 20%, while TS keeps invariable.

The pre-strain effect on the deterioration of HDR is shown in **Fig.4**. The pre-strain of 40% reduces the increase of M100 due to the thermal oxidation from 200% to 125%. EB and TS do not seem to be affected. In the ozone test, the low-temperature ozone test, the salt water and the acid rain mist combined cycle test, the pre-strain strengthens the ageing effects, making M100 increase more, EB decrease more. Especially in the ozone test, EB decreases by more than 4 times, and M100 increases by nearly twice. In the acid rain mist combined cycle test, the change of M100 and EB with the 40% pre-strain is more than twice of that without pre-strain

In general, thermal oxidation affects rubber properties much greater than other factors such as ozone, ozone in low temperature, salt water and acid rain. Ultraviolet radiation also changes material properties greatly. However, it can only reach the surface of rubber bearing, while oxygen can permeate into the interior. It is therefore reasonable to deem thermal

oxidation as the dominant degradation factor. Attention should be paid to the phenomenon that in the thermal oxidation, the increase of M100 is found to be lessened by the pre-strain.

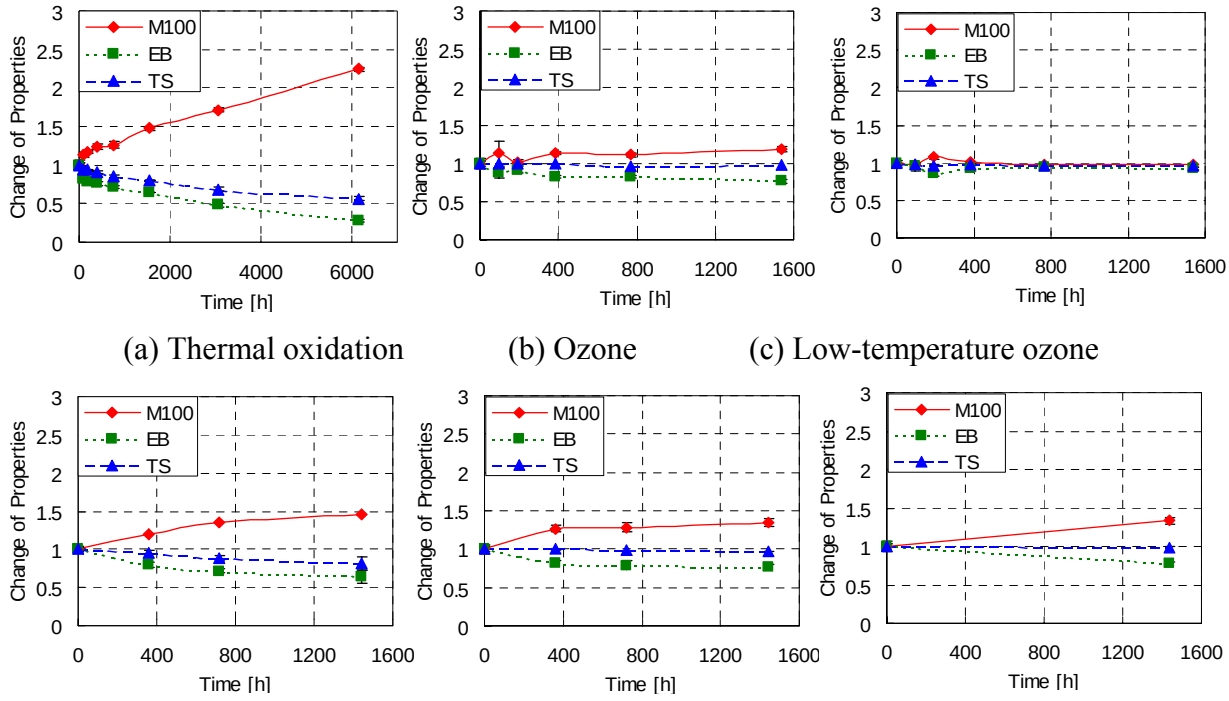

(a) Thermal oxidation (b) Ozone (c) Low-temperature ozone

(d) Ultraviolet radiation (e) Salt water combined cycle (f) Acid rain

Fig. 3 Relative property changes of HDR (pre-strain = 40%)

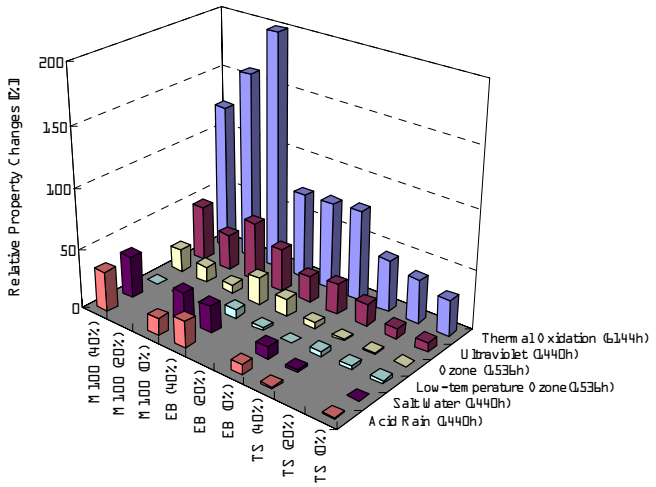

Fig. 4 Effect of pre-strain on aging of HDR material

3. ACCELERATED THERMAL OXIDATION TESTS ON HDR BLOCK

Among different degradation factors such as oxidation, ultraviolet radiation, ozone, temperature, acid and humidity, it is found that thermal oxidation changes the HDR properties more greatly than other factors, resulting in an increase of HDR's stiffness and a decreases of elongation at break as well as tensile strength. Besides, for thick rubbers, it is obvious that the surface is more easily affected by deterioration factors than the interior because of the diffusion-limited oxidation effect (Celia et al., 2000; Wise et al., 1997). In order to understand the variation of the material property inside the HDR bearings, accelerated tests were performed using rubber blocks using the dominant degradation factor, thermal oxidation. The test method and results are described as follows.

3.1 Specimens and Test Methods

Fifteen HDR blocks are used as test specimens, as shown in **Fig.5**. The dimension is 220×150×50mm (length×width×thickness). The specimens are accelerated aged in a Thermal Ageing Geer Oven. The test conditions are listed in **Table 2**. Three elevated temperatures, 60□, 70□, and 80□ are applied in the oven. For the test under each temperature, the experiment duration are set as 5 stages, with the maximum lasting of 300 days **Fig.6** shows the accelerated thermal oxidation test flow. When the rubber block specimen is taken out from the oven, it is sliced into pieces with a thickness of 2mm.

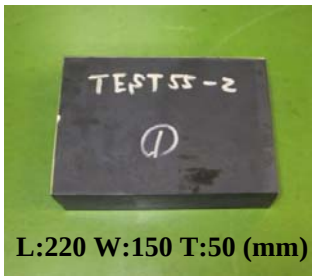

Fig.5 Rubber block specimen

Table 2 Accelerated thermal oxidation test condition

Temperature ( )	Test Duration (days)
60	31 , 60 , 100 , 200 , 300
70	12 , 22 , 38 , 75 , 113
80	4 , 8 , 14 , 28 , 42

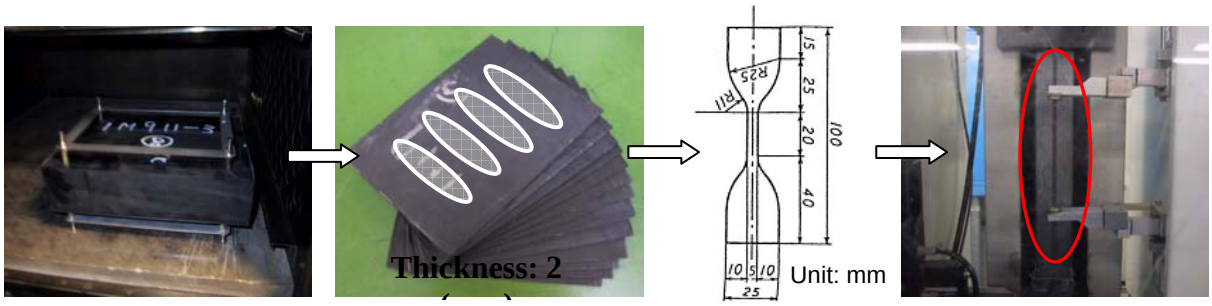

(a) Accelerated test *(b) Rubber slices* (c) No.3 dumbbell *(d) Tensile test*

Fig.6 Accelerated thermal oxidation test flow

From each slice, four specimens with No.3 dumbbell shape are cut out. And there are more than 3,000 samples in total. Then through the tensile tests on these dumbbell specimens, the stress-strain curves can be obtained, which represent the rubber properties at the corresponding position.

In this research, strain energy is chosen for examination for the reason that it can exhibit the effect of thermal oxidation more remarkably than stresses at certain strains. In the

following description, the strain energy corresponding to the strain of 100% is called U100, the strain energy up to the break is called UB, and the modulus of the stress corresponding to the strain of 100% is called M100. Similarly, the distribution of U100 inside rubber blocks is called U100 profile, and the distribution of mechanical properties like modulus, elongation at break (EB) and tensile strength (TS) is called property profile.

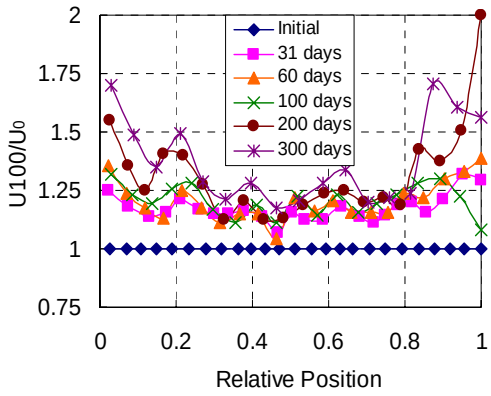

(a) 60□

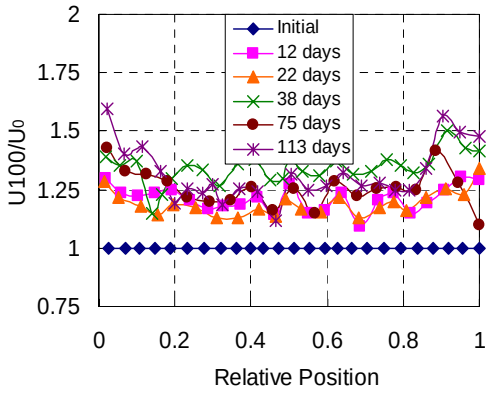

(b) 70□

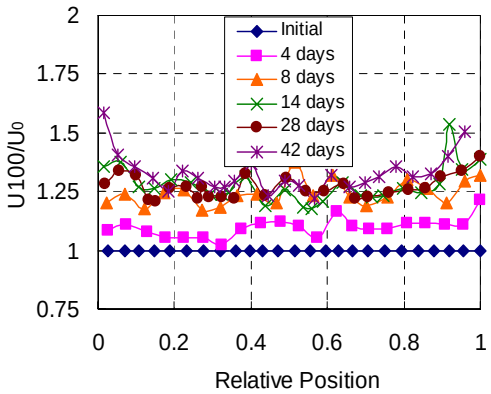

(c) 80□

Fig.7 $U100/U_0$ profile

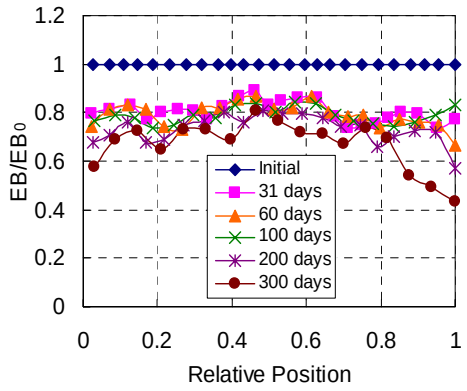

(a) 60□

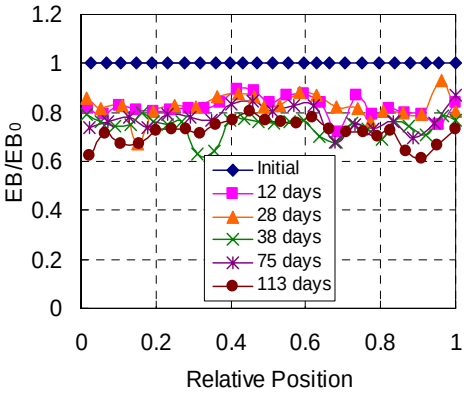

(b) 70□

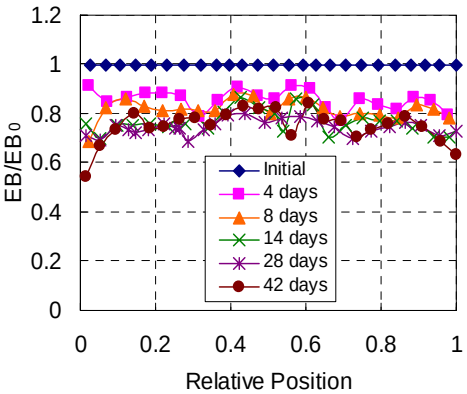

(c) 80□

Fig.8 EB/EB_0 profile

3.2 Test Results and Discussions

The profiles of $U100/U_0$ and EB/EB_0 at every test temperature are illustrated in **Fig.7** and **Fig.8**, respectively. The horizontal axis shows the relative position with regard to the thickness of HDR block. The values 0 and 1 on this axis correspond to the surface of the block. The vertical axis shows the normalized change of U100 with the original value regarded as 1.00 in **Fig.7**, and shows the normalized change of elongation at break in **Fig.8**. In these figures, every point represents the mean value of four specimens from the same slice. Because of the unevenness of rubber materials, at any position four specimens are tested in order to improve the accuracy. Since the oxidized rubber inhibits the ingress of oxygen, and considering the shape of the rubber block, the four specimens are cut out from the area at least 25mm, a half of the block thickness, away from the around surface. Thus these specimens only reflect the property variations in the thickness direction. The standard deviation of every four-specimen group is quite small and usually less than 5% of the mean value.

From **Fig.7** and **Fig.8**, it can be found that at the early stage of the test, the material properties in the outside region change together with the interior regions. The property variation of the interior region soon reaches the equilibrium state and becomes stable. However, the properties near the surface keep changing over the time and they change most greatly at the surface. From the surface to the interior, the properties vary less and less, until to a certain depth, which is called "critical depth". The critical depth is about 11.5mm from the block surface at 60□, 8.5mm at 70□, and 6mm under 80□.

Fig.9 shows the time dependency of U100 and EB at the surface and in the interior of HDR blocks. The horizontal axis shows the deterioration time, and the vertical axis shows the material property variations compared to its initial state. The data of the block surface are taken from the top and the bottom surfaces, while the data of the block interior are taken from two slices close to the middle piece. Therefore, there are 8 points corresponding to each time. From **Figs.9(a)** and **9(c)** it is found that U100 and elongation at break at the block surface change nonlinearly over the time. In **Figs.9(b)** and **9(d),** the property variation in the interior region occurs in a very short time, then becomes stable. U100 increases by 20□40% and elongation at break decreases by about 20%.

From the test results, it can be said that the deterioration characteristics of HDR block can be observed in two regions; one is in the interior region beyond the critical depth, where the properties only change at the early stage, the other is in the outer region from the surface to the critical depth, where the properties continue changing after a rapid initial change. Since the deteriorated rubber is considered to inhibit the diffusion of oxygen, oxidation deterioration can only progress to a certain depth and the interior region beyond the critical depth is not affected by oxygen. The oxidation is a process related to the time but the property variation in the interior region completes in very short time. It should be a spontaneous reaction in the interior region of HDR block. Because the property variation in this region increases with temperature, it is assumed the region beyond the critical depth is only affected by temperature. Therefore, it is thought that there are two kinds of reaction in the aging of the HDR material, spontaneous reaction and oxidation. The interior region is only affected by spontaneous reaction, and this reaction completes in a relatively short time. However, for the outer region near the surface, spontaneous reaction and oxidation affect HDR simultaneously. After the spontaneous reaction reaches the stable state, only the oxidation deterioration continues.

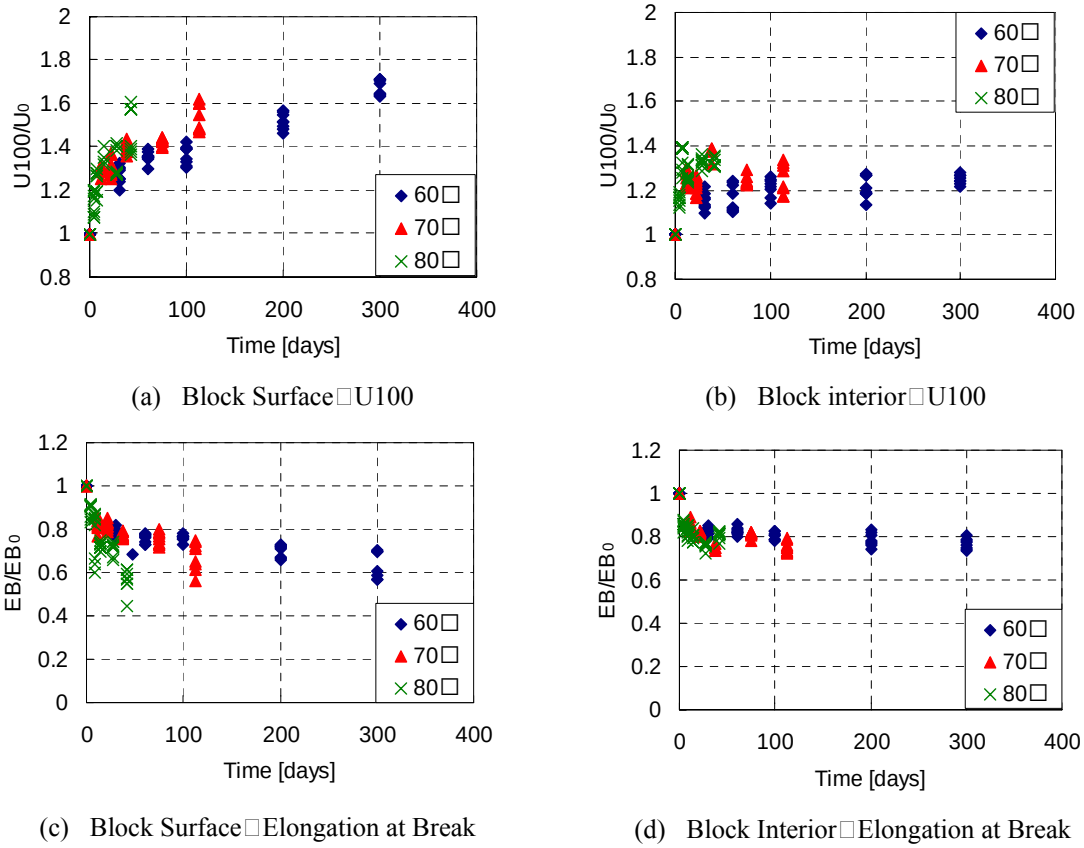

(a) Block Surface□U100 (b) Block interior□U100

(c) Block Surface□Elongation at Break (d) Block Interior□Elongation at Break

Fig.9 Time Dependency of U100 and elongation at break

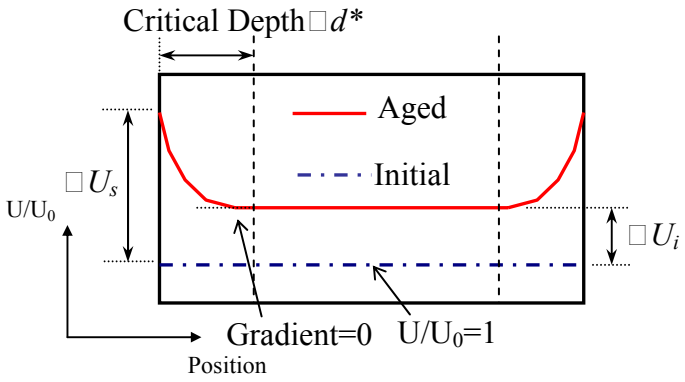

Fig.10 Strain energy profile pattern

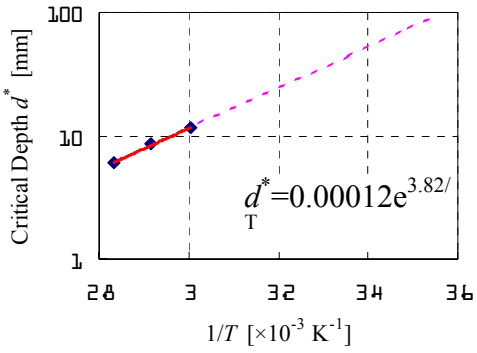

Fig.11 Relations between critical depth and temperature

4. AGING MODEL FOR HDR BRIDGE BEARING

In order to predict the long-term deterioration of HDR bridge bearing, it is necessary to quantify the deterioration characteristics. Based on the accelerated thermal oxidation test results show in **Figs.7□9**, the deterioration pattern of the HDR block can be schematically expressed by **Fig.10**. The vertical axis U/U_0 means the relative property change, which is the ratio of the current material property U comparing to the original value U_0. The horizontal axis shows the relative position inside the HDR block. The spontaneous reaction in the

interior region beyond the critical depth d^* is only affected by temperature, and the relative property variation is ΔU_i. The outer region from surface to the critical depth d^* is influenced by both spontaneous reaction and oxidation, and the property changes most greatly near the block surface. The relative property variation at the bearing surface is represented by the symbol of ΔU_s. When proceeding into the block, because of the decrease in the amount of oxygen, the oxidation effect becomes weaker, and the property variation also declines. Once exceeding the critical depth, the gradient of the property profile becomes zero.

4.1 Critical Depth

Muramatsu et al. (1995) has discovered that the critical depth is an exponential function of the reciprocal of the absolute temperature as following.

$$d^* = \alpha \exp\left(\frac{\beta}{T}\right) \tag{1}$$

where, d^* is the critical depth, T is the absolute temperature, and the symbols α and β are coefficients determined by the ageing test.

The exponential relationship between the critical depth and the temperature is verified in **Fig.11**. In this figure it is found that for the HDR in this test, α=0.00012mm, β=3.82×10^{-3}.

4.2 Property Variation of Interior Region

The test results show that the interior region changes in relatively very short time, and then keeps stable. It changes so rapidly that the time-dependency may be neglected. EB decreases about 20% no matter under what temperature. However, the equilibrium state of strain energy is correlated with temperature, as shown in **Fig.12**. The relationship between the temperature and the strain energy variation in the interior region may be expressed by an exponential function as follows:

$$\Delta U_i = A \exp\left(\frac{B}{T}\right) \tag{2}$$

Where, ΔU_i is the relative strain energy variation of the interior region, T is the absolute temperature, and the symbols A and B are coefficients.

The symbols A and B in Eq.(2) are found to be related to the nominal strain. The strain-dependency is observed in **Fig.13**, in which the coefficients A and B versus the strain from 25% to 500% are plotted, and they can be calculated approximately using the following equations.

$$\ln A = b_1 \ln \varepsilon + b_2 \tag{3a}$$

$$B = c_1 \ln \varepsilon + c_2 \tag{3b}$$

where, ε is the nominal strain, the symbols b_1, b_2, c_1, and c_2 are factors determined by the tests.

4.3 Property Variation at Block Surface

The property variation at the block surface can be deemed as the combined effect of spontaneous reaction and oxidation. Temperature not only affects the degree of the spontaneous reaction, but also accelerates the oxidation reaction.

Figs.14(a) and **14(b)** show the relative change of U100 and elongation at break at the bearing surface with the property variations at 60□. At a certain temperature, the property of HDR exposed to the air depends on the time. It is also found that the increase of U100 and the decrease of elongation at break are linear with the aging time. For other material properties, the similar relationship is proved. The time dependency can be expressed by the following equation:

$$U_s' / U_{s0} = k_s \cdot t + 1 \qquad (4a)$$

where, U'_s/ U_{s0} is the relative variation of strain energy at the surface of the rubber bearing due to the oxidation only, k_s is coefficient and t is the deterioration time.

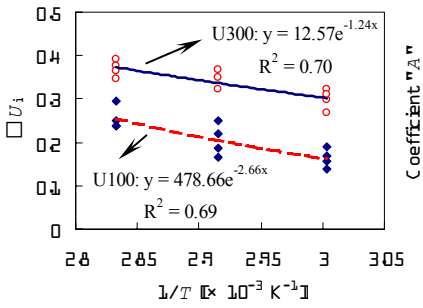

Fig.12 Relations between inner strain energy change and temperature (60□)

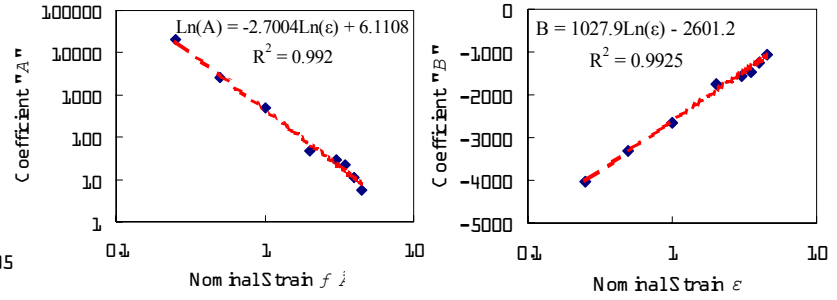

***(a)** Coefficient "A"* ***(b)** Coefficient "B"*

Fig.13 Relations between coefficient "A", "B" and nominal strainε

The relative property variation at the bearing surface also depends on strain. The relation between the coefficient k_s and the nominal strain $\varepsilon$is shown in **Fig.15**, and the following equation can be obtained.

$$k_s = a_1 \cdot \varepsilon + a_2 \qquad (4b)$$

where, a_1 and a_2 are the factors determined by the test.

Since the normalized property variation at the bearing surfaceΔU_s is affected by the aging effects due to both the spontaneous reaction and the oxidation, the following equation is obtained.

$$\Delta U_s = (1 + k_s \cdot t) \cdot (1 + \Delta U_i) - 1 \qquad (4c)$$

4.4 Aging Model of HDR Bearing

A simple equation is necessary to express the property variation in the region from the rubber bearing surface to the critical depth. The property variation $U(t)/U_0$ should be the function of the position x. The boundary conditions are:

$$\begin{cases} U(t)/U_0=1+\Delta U_s \ (x=0 \text{ or } l) & (5a) \\ U(t)/U_0=1+\Delta U_i \ (d^*\le x\le l-d^*) & (5b) \\ dU(t)/dx=0 \qquad (x=d^*) & (5c) \end{cases}$$

where, $U(t)$ and U_0 are the HDR properties at time t and the initial state, respectively. ΔU_i andΔU_s are the relative property changes of the interior region and the bearing surface, respectively. d^* is the critical depth, and l is the width of the HDR bearing.

If the property variation $U(t)/U_0$ is assumed to be a square relation of the position x, the function can be expressed as follows:

$$U(t)/U_0=a_1x^2+a_2x+a_3 \quad (6)$$

Considering the boundary conditions Eq.(6) can be written as:

$$\frac{U(t)}{U_0}=1+\left[w\Delta U_s+(1-w)\Delta U_i\right] \quad (7)$$

$$w=\begin{cases} \left(\dfrac{x-d^*}{d^*}\right)^2 & (0\le x\le d^*) \\ 0 & (d^*\le x\le l-d^*) \\ \left(\dfrac{x-(l-d^*)}{d^*}\right)^2 & (l-d^*\le x\le l) \end{cases} \quad (8)$$

where, w is the coefficient correlated with the position x, the critical depth d^* and the width l of the HDR bearing.

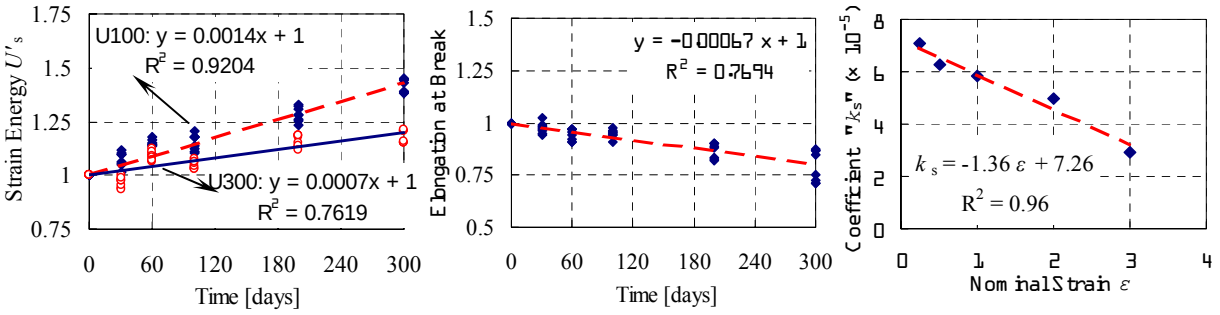

(a) Strain energy (b) Elongation at break

Fig.14 Time dependency of HDR block surface (60□)

Fig.15 Relations between strain and coefficient "k_s" (HDR, 60□)

4.5 Verification of The Aging Model

Based on the test results, the coefficients in the equations mentioned above are deduced and presented in Table 3. Through the comparisons shown in Fig.16, it is found that the simulations of the critical depth, the property variation at the block surface and in the interior

agree well with the test results. Thus the feasibility of the deterioration assessment method is verified.

Table 3 Parameters of deterioration prediction model (60□)

α [10^{-4}mm]	β [$10^{3}K^{-1}$]	[10^{-5}]	[10^{-5}]	[10^{-5}]	[10^{-5}]	b_1	b_2	c_1 [10^{3}]	c [10^{3}]	k_{bs} [10^{-3}]	E_{bi}
1.21	3.82	-0.12	0.42	-1.63	7.24	-2.70	6.11	1.03	-2.60	-0.67	-0.20

*k_{bs}: Change rate of EB on block surface **□E_{bi}: Change of EB in the interior

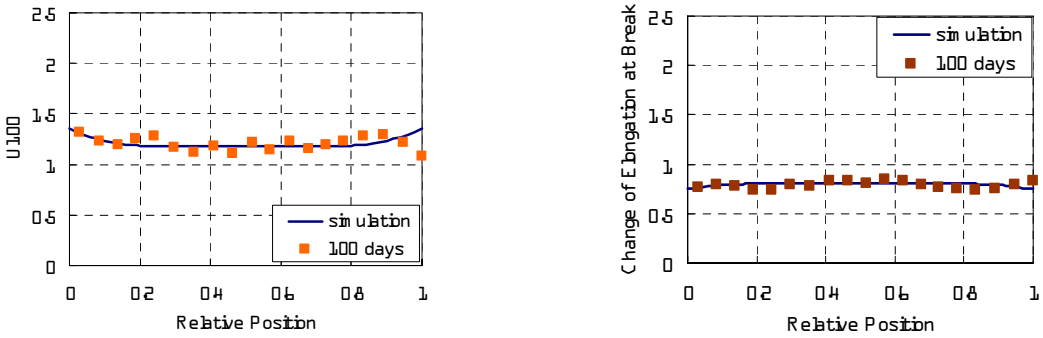

(a) U100 (b) EB

Fig.16 Comparison between test results and simulation (60□)

4.6 Activation Energy

In the thermal oxidation test the temperature is much higher than the temperature in the real environment because high temperature can accelerate the deterioration. Using the Arrhenius methodology, the accelerated ageing results could be correlated with ageing under service conditions (Wise et al., 1995). The deterioration time in the accelerated exposure tests can be converted into the service conditions through Eq.(9), then the deterioration of bridge rubber bearing under service conditions can be assessed based on the accelerated thermal oxidation tests.

$$\ln(\frac{t_r}{t}) = \frac{E_a}{R}(\frac{1}{T_r} - \frac{1}{T}) \qquad (9)$$

where, E_a is the activation energy of rubber, R is the gaseous constant (=8.314[J/mol·K]), T_r indicates the absolute temperature in the service condition, and T is the absolute temperature in the thermal oxidation test. The symbols t_r and t are the actual time and test time, respectively.

Since the rubber surface contacts with the air, the surface is thought completely oxidized. Therefore, the time-dependency of properties at the surface are used to determine the activation energy, for example, the data in **Fig.9(a)** and **Fig.9(c)**. The principle of time/temperature superposition by shifting the raw data to a selected reference temperature T_{ref} is employed (Wise et al., 1995). This principle is shown in **Fig.17**. In this study, the reference temperature is chosen as 60□ and the curve at 60□ is the master curve. The shift

factors a_T are chosen to give the best superposition of the data. If the data adhere to an Arrhenius relation, the set of the shift factors a_T will be related to the Arrhenius activation energy E_a by the following expression:

$$a_T = \exp\frac{E_a}{R}\left(\frac{1}{T_{ref}} - \frac{1}{T}\right) \qquad (10)$$

The activation energy is calculated and listed in **Table 4**. The average value of E_a is about 9.04×10^4[J/mol]. Then using the Arrhenius methodology, the property variations of HDR under any service condition may be predicted based on the accelerated thermal oxidation test results.

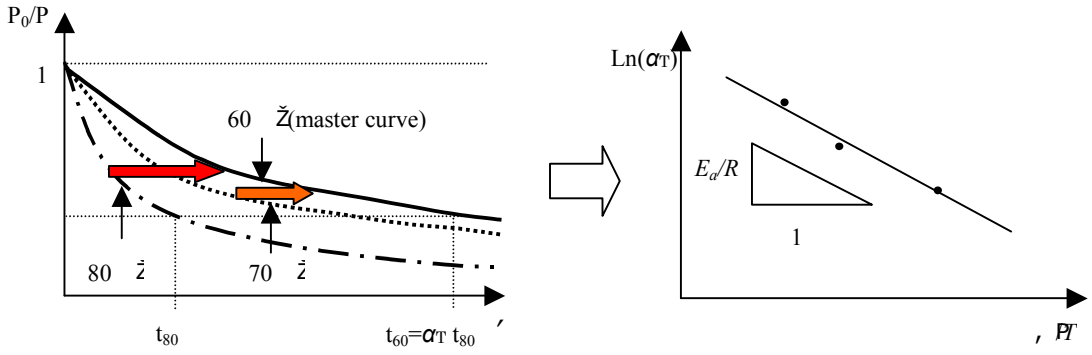

Fig. 17 Principle of time/temperature superposition to obtain activation energy

Table 4 Activation energy of HDR

HDR Property	U25	U50	U100	U200	U300	UB	EB	Averag
E_a ($\times10^4$J/mol)	8.97	8.90	8.84	8.23	7.61	9.93	1.08	9.04

UB: Strain energy at break
EB: Elongation at break

5. LONG-TERM PERFORMANCE OF HDR BRIDGE BEARING

5.1 FEM Model and Analytical Conditions

Using the constitutive model of HDR materials proposed by Yoshida et al.(2004), HDR bridge bearings are modeled with a three-dimensional finite elements methodology (Itoh et al., 2006), as shown in **Fig.18**. The basic information of the FEM model is listed in **Table 5**. The coating rubber is 10mm, which is manufactured together with the main body during the molding process. Thus, the coating rubber also contributes to the shear force. The critical depth is calculated from the surface of the coating rubber.

Firstly the deterioration prediction model gives the property profiles of aged HDR bridge bearing. Then, the parameters of the constitutive model are determined by the predicted properties using the Genetic Algorithm (GA). These parameters are used to define the HDR elements at the corresponding position in the FEM model (ABAQUS, 2004). Since it was estimated that the change in material properties between the surface and the critical depth would be more outstanding than that in other regions, this region is meshed finely. In Japan,

the yearly average temperature varies from 5.4□ to 24□, and the maximum critical depth is nearly 120mm according to Eq.(1). The periphery with a thickness of 120mm is finely meshed.

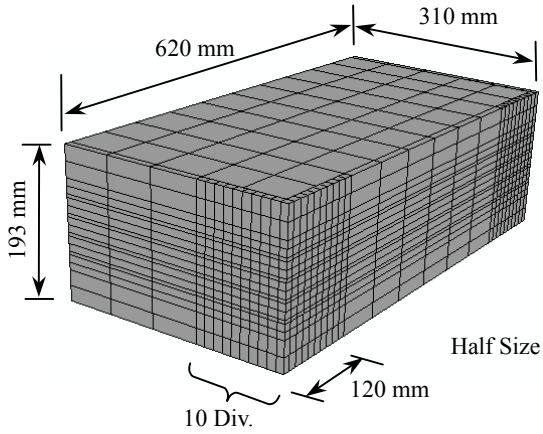

Fig. 18 FEM model of HDR bearing

Table 5 Parameters of FEM model

Bearing size [mm]	600×600
Thickness of rubber layer [mm]	19
Thickness of steel plate [mm]	4.5
Thickness of coating rubber [mm]	10.0
Number of rubber layers	5
Number of steel plates	4
The 1st shape factor	7.89
Number of Nodes	10,650
Number of Elements	4,080

It is known if the model is meshed more finely, the result will be more accurate, however, the time required for computing will be much longer. In order to get enough precise resolution within a reasonable time, the influence of the mesh size is investigated. As shown in **Fig.19**, the outer region is divided into 5, 10 and 20 layers. It can be seen that the difference when the divided layers are 10 and 20 is only about 1%. Therefore, 10 dividing of the outer region are thought to be able to yield good accuracy.

In order to get the shear stiffness of HDR bridge bearing, the FEM model is analyzed in simulation following the conditions shown in **Fig.20**. The loading conditions conform to the *Manual of Highway Bridge Bearing* (JRA, 2004). A constant vertical force is loaded to the upper plane of the bearing while keeping the upper and lower planes horizontal. The nodal displacements are constrained to ±166.3mm, which corresponds to ±175% of shear strain. Two cycles of sine wave are inputted at 0.5Hz.

Considering the yearly average temperature in Japan and the common bridge lifespan, the following cases are analyzed. The temperatures are assumed to be 5□, 10□, 15□, 20□ and 25□. The deterioration time considered is from 0 year to 100 years with an interval of 20 years. Including the case in the initial state, totally there are totally 26 deterioration cases analyzed.

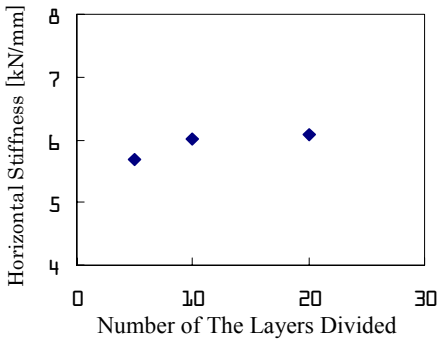

Fig. 19 Influence of mesh size

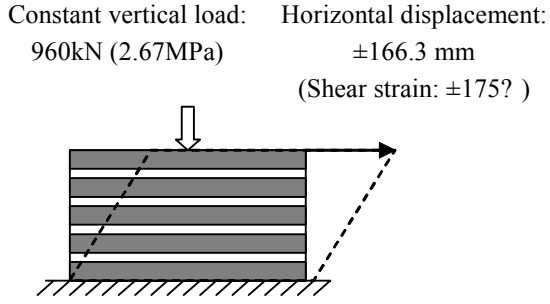

Fig. 20 Loading condition of FEM analysis

5.2 FEM Analysis Results

From the hysteretic loops obtained from FEM analysis, the equivalent horizontal stiffness and the equivalent hysteretic damping ratio can be obtained. The influences of time and temperature are investigated.

Fig.21 shows the time-dependency of the equivalent horizontal stiffness and the equivalent damping ratio of 600 mm square HDR bridge bearing. The values are normalized by taking the initial properties as 1.00. In **Fig.21(a)**, generally the equivalent horizontal stiffness increases over the time, and it increases much faster during the early stage of application. When the property variation due to the temperature stops, the increasing speed slows down. After 100 years, the equivalent horizontal stiffness increases more than 20% of 25□. However, of 5□ and 10□, it only increases by about 10%. In this figure, the irregularity of the tendency is the result of the errors during the definition of parameters in the constitutive model, which accumulated and behaved themselves in the FEM results. Moreover, in this study only the uniaxial test is performed, it is difficult to precisely predict the equivalent damping ratio for hyperlinear HDR material, but the variation tendency can be at least obtained. From **Fig.21(b)**, it is found the equivalent damping ratios show a small increase soon after the HDR bearing is applied, then decrease over the time. However, after 100 years the equivalent damping ratio is not estimated to change much, and remains within the range of ±5%.

Fig.22 shows the temperature-dependency of the equivalent horizontal stiffness and the equivalent damping ratio. It is clear that the equivalent horizontal stiffness increases more greatly at a higher temperature. However, the effect of temperature is small when below 10□. After 60 years, the increase of the equivalent horizontal stiffness at 25□ is estimated to be twice as high as that at 5□ or 10□. On the other hand, there seems no apparent correlation between the equivalent damping ratio and the temperature, and the variations among different analyzed temperatures are very small and remains within 5%.

It can be concluded that the equivalent horizontal stiffness increases rapidly during the early service stage until the reaction due to the temperature reaches the equilibrium state, and then the increase speed slows down. In the second stage it increases faster at higher temperatures. After 100 years the equivalent horizontal stiffness of a 600 mm square HDR bridge bearing is estimated to increase by about 10□25%. As to the equivalent damping ratio, it declines slowly after a small increase during the early stage. After 100 years it is estimated to change within ±5% and shows no relations with temperature.

Following the aforementioned procedure, the property profiles of a HDR bearing with any size can be estimated using the deterioration prediction model, and the performance can be obtained through the similar FEM analysis. Since in a larger HDR bearing, the proportion of the outer region, where the property changes more greatly, to the whole area is less, the equivalent horizontal stiffness will change less than a smaller HDR bearing. However, because the spontaneous reaction occurs in the whole HDR bearing, the material properties change evenly in the early stage before the aging due to the oxidation behaving itself, and the variation is only related to the temperature. Therefore, the initial variation of the equivalent horizontal stiffness due to the temperature does not make any difference for different sizes.

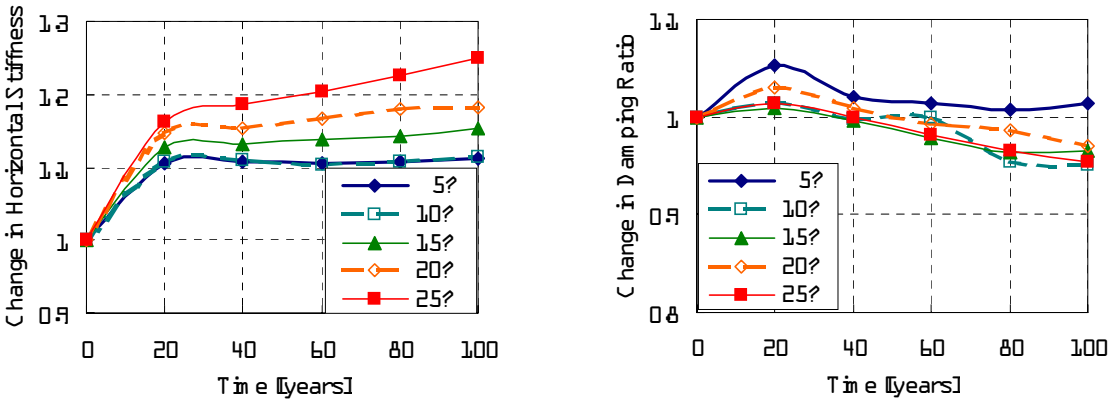

(a) Equivalent horizontal stiffness (b) Equivalent damping

Fig. 21 Time-dependency of the performance of HDR bridge bearing (600×600 mm)

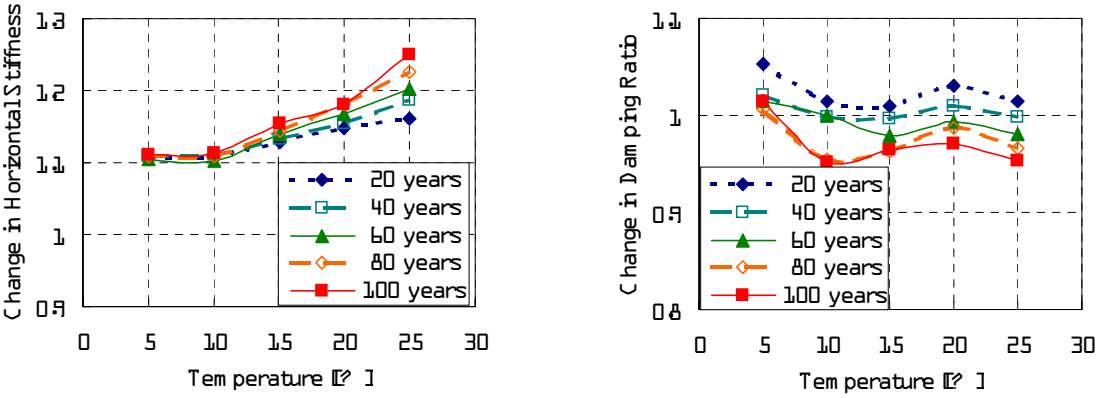

(a) Equivalent horizontal stiffness (b) Equivalent damping

Fig. 22 Temperature-dependency of the performance of HDR bridge bearing (600×600 mm)

6. CONCLUSIONS

In this research, accelerated exposure tests are firstly carried out using various degradation factor. Then the accelerated tests are performed on HDR blocks using thermal oxidation, which is the dominant degradation factor. The deterioration characteristics inside the blocks are investigated. Based on the test results, an aging models is proposed for HDR bridge bearings. Finally, Then, the long-term performance of the HDR bridge bearing is investigated through FEM analysis by estimating the future property profiles using the proposed aging model. The major findings and conclusions are summarized as follows:

1. The thermal oxidation is discovered to be the most significant degradation factor, due to which the stress corresponding to 100% strain (M100) of HDR experiences an increase of more than 200% over long time, while tensile stress decreases to nearly 50% and elongation at break decreases to only 25%.
2. For those insignificant degradation factors the stable state is reached in the early time and the property changes are usually less than 50%. The aging effect causing the increase of modulus would be lessened by the pre-strain.
3. The material properties of HDR blocks display the features of a diffusion-limited oxidation: initially the profiles are relatively homogeneous, but strong heterogeneity develops with ageing. The outer region changes more than the interior region.

4. From the block surface to the interior, the property variations decrease gradually until to the critical depth. The interior of HDR block becomes invariable after a sudden change.
5. Based on the test results, the relationships among property change, temperature, position, and strain are quantatified. An aging model for HDR bridge bearing is proposed, which can estimate the property profiles of aged bridge rubber bearings. Combined with the Arrhenius methodology, the deterioration characteristics under service conditions may be predicted.
6. Through FEM analysis of 600 mm square HDR bridge bearing, it is found that the equivalent horizontal stiffness increases gradually after a rapid increase during the early service stage. After 100 years it is estimated to increase by about 10□25%. At a higher temperature, the increase speed becomes faster. However, the equivalent damping ratio decreases over the time, and seems to have no relation with the temperature. The variation is only about only ±5%.

7. REFERENCE

ABAQUS□Standard ver.6.4 USER'S MANUAL, 2004□

Celia M., Wise J., Ottesen D. K., Gillen K. T. and Clough R. L., 2000, *Correlation of chemical and mechanical property changes during oxidative degradation of neoprene*, Polymer Degradation and Stability, Vol. 68, 2000, pp171-184

Itoh, Y., Satoh, K., Gu, H. S. and Yamamoto, Y., 2006, *Study on the deterioration characteristics of natural rubber bearings*, Journal of Structural Mechanics and Earthquake Engineering, JSCE, Vol.62, No.2

JRA, 2004, *Manual of highway bridge bearing*, Japan Road Association, 2004, p.200 (in Japanese)

Muramatsu Y. and Nishikawa I., 1995, *A study for the prediction of the long-term durability of seismic isolators*, Showa electric wire review, Vol. 45, No.1, 1995, pp44-49 (in Japanese)

Sudoh, C., Nishi, T., Shimada, G., Yazaki, F. and Okutsu, N., 2003, *Performance evaluation and inner property profile of isolators used for 10 years*, Proceedings of Annual Conference of the Japan Society of Civil Engineers, Vol. 58, 2003, pp763-764 (in Japanese)

Wise J., Gillen K. T., and Clough R. L., 1995, *An ultrasensitive technique for testing Arrhenius extrapolation assumption for thermally aged elastomers*, Polymer Degradation and Stability, Vol. 49, Issue. 3, 1995, pp403-418

Wise, J., Gillen, K. T. and Clough, R. L., 1997, *Quantitative model for the time development of diffusion-limited oxidation profiles*, Polymer, Vol. 38, No. 8, 1997, pp.1929-1944

Yoshida, J., Abe, M. and Fujino, Y., 2004, *Constitutive model of high-damping rubber materials*, Journal of Engineering Mechanics, ASCE, Vol. 130, No. 2, 2004, pp129-141

Yoshida, J., Abe, M. and Fujino, Y., 2004, *Three-dimensional finite-element analysis of high damping rubber bearings*, Journal of Engineering Mechanics, ASCE, Vol. 130, No. 5, 2004, pp607-620